Supporting Information

Mixing and Matching Detergents for Membrane Protein NMR Structure Determination

Linda Columbus, Jan Lipfert, Kalyani Jambunathan, Daniel A. Fox, Adelene Y. L. Sim,

Sebastian Doniach, & Scott A. Lesley

Figure S1. The structure of the nitroxide probe.

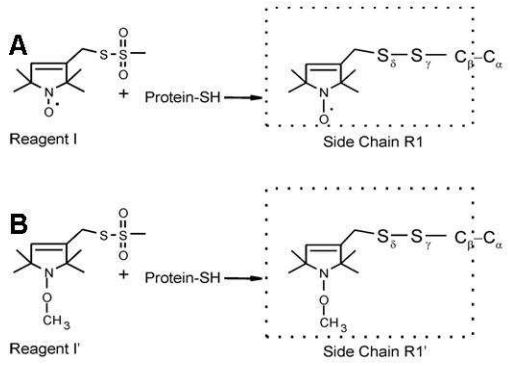

Reactions of labeling reagents RI and RI' with a protein sulfhydryl group to generate the corresponding side chains R1 and R1'. The **R1** side chain is the most extensively characterized nitroxide side chain and has been introduced into many protein sequences[1-4]. The R1' side chain is the diamagnetic equivalent to the paramagnetic R1 side chain.

Figure S2. The introduction of nitroxide spin labels does not perturb the overall fold of TM0026.

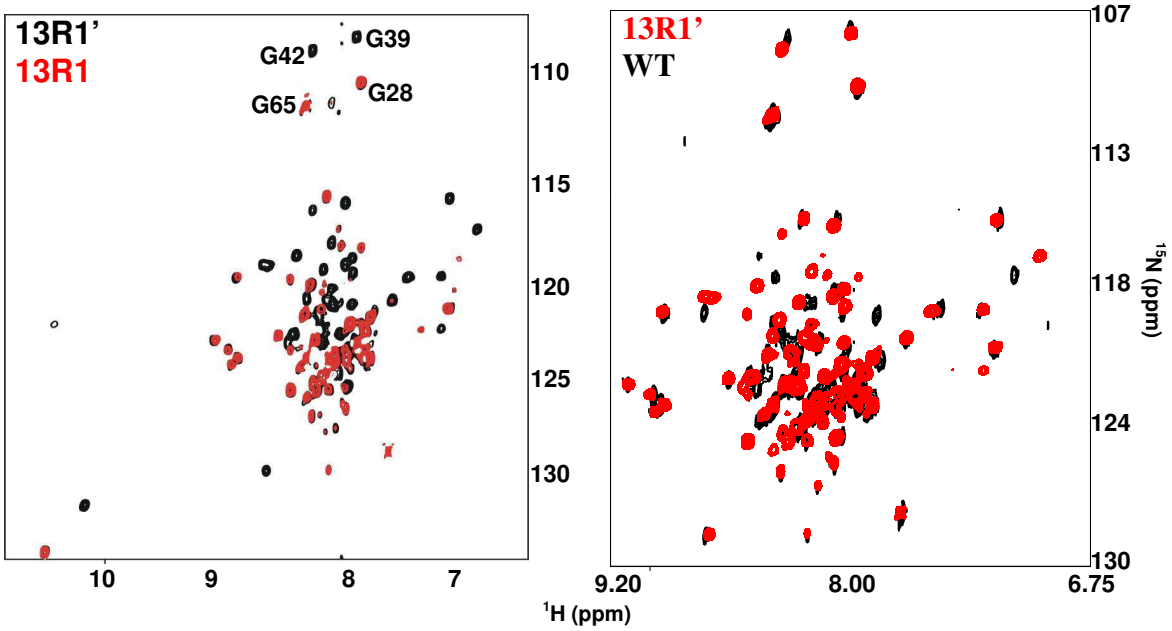

^{15}N, ^{1}H-TROSY spectra of A13R1, A13R1', and wild type TM0026 in the FC-10/DDM mixed micelle. With the ^{2}H,^{15}N-labeled protein the fold of the labeled protein can be assessed based on the ^{15}N-TROSY spectrum. However, the **R1** side chain is paramagnetic and enhances the relaxation of neighboring protons in a distance dependent manner, thus obliterating some of the cross-peaks in the ^{15}N-TROSY spectrum. To circumvent this effect, a diamagnetic analog (**R1'**, **Figure S1**) was also introduced at A13, which is isosteric to **R1**, but will not enhance the relaxation of neighboring protons. The spectra of A13R1 and A13R1' are super-imposable for the observed resonances. The missing cross-peaks in A13R1 are due to relaxation enhancement as a result of the paramagnetic side chain. The spectra of A13R1' and wild type are superimposable with some subtle chemical shifts of resonance that are adjacent to the nitroxide side chain. The A13R1' cross-peak is severely shifted and could not be assigned.

Figure S3: Detergent structures.

a

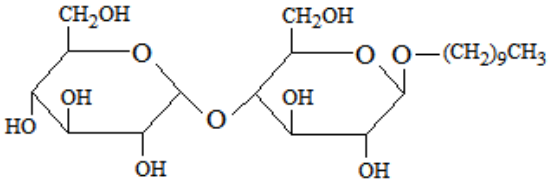

b

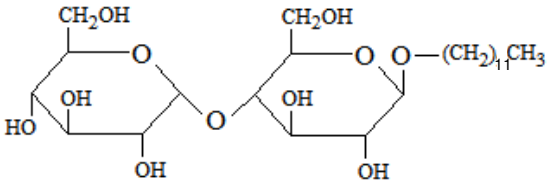

c

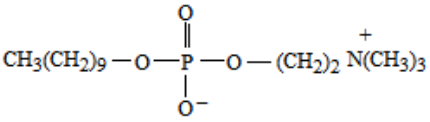

d

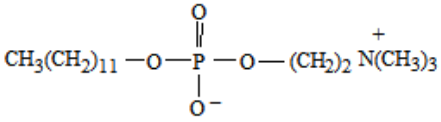

e

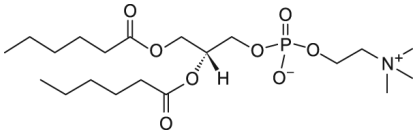

f

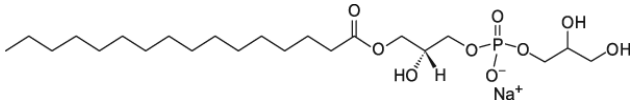

The chemical structures of (a) DM, (b) DDM, (c) FC-10, (d) FC-12, (e) DHPC, and (f) LPPG.

Figure S4. SAXS data for FC-10/DDM and DHPC/LPPG mixed micelles.

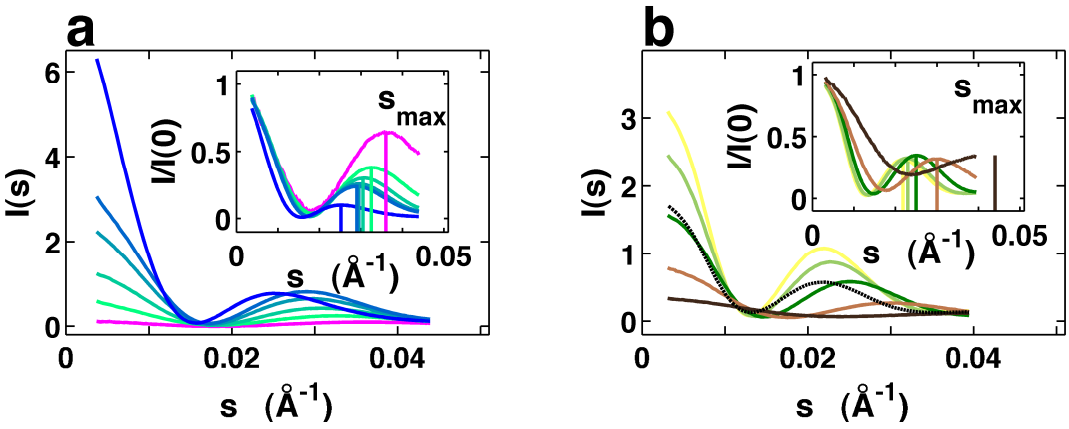

Small-angle X-ray scattering profiles for FC-10/DDM and DHPC/LPPG mixed micelles. Scattering intensities are shown as a function of momentum transfer s ($s = 2\sin(\theta)/\lambda$, where 2θ is the total scattering angle and λ is the X-ray wavelength). (a) Data for 50 mM FC-10 (magenta), 50 mM DDM (blue) and for FC-10/DDM mixtures of 50/10 mM (light green), 50/25 mM (cyan), 50/40 mM (green-blue), 50/50 mM (light blue). (b) Data for 50 mM DHPC (dark brown), 50 mM LPPG (yellow) and for DHPC/LPPG mixtures of 10/40 mM (light green), 25/25 mM (green), 40/10 mM (light brown). Significant mixing between the detergents is observed since the scattering profile of the 1:1 mixtures (light blue in panel a and green in panel b) are not equal to the sum of the pure FC-10 (a, magenta) and DDM (a, blue) or to the sum of pure DHPC and LPPG scattering profiles (shown as a black dashed line in panel b). The inset shows the same profiles normalized by forward scattering intensity I(0). The positions of the characteristic second maximum in the scattering intensity, s_{max}, for the different compositions are denoted by the vertical lines in the inset. The second maximum in the scattering profile of micelles is due to the interference of the head group scattering across the hydrophobic micelle core[1]. $1/s_{max}$ corresponds to the head group-head group spacing L across the short dimension of the spheroid micelle core[1], see Figure S5. The position of the second peak for pure DHPC (panel b), dark brown) was taken from reference[5].

Figure S5. Two-component ellipsoid models for FC-10/DDM and DHPC/LPPG mixed micelles.

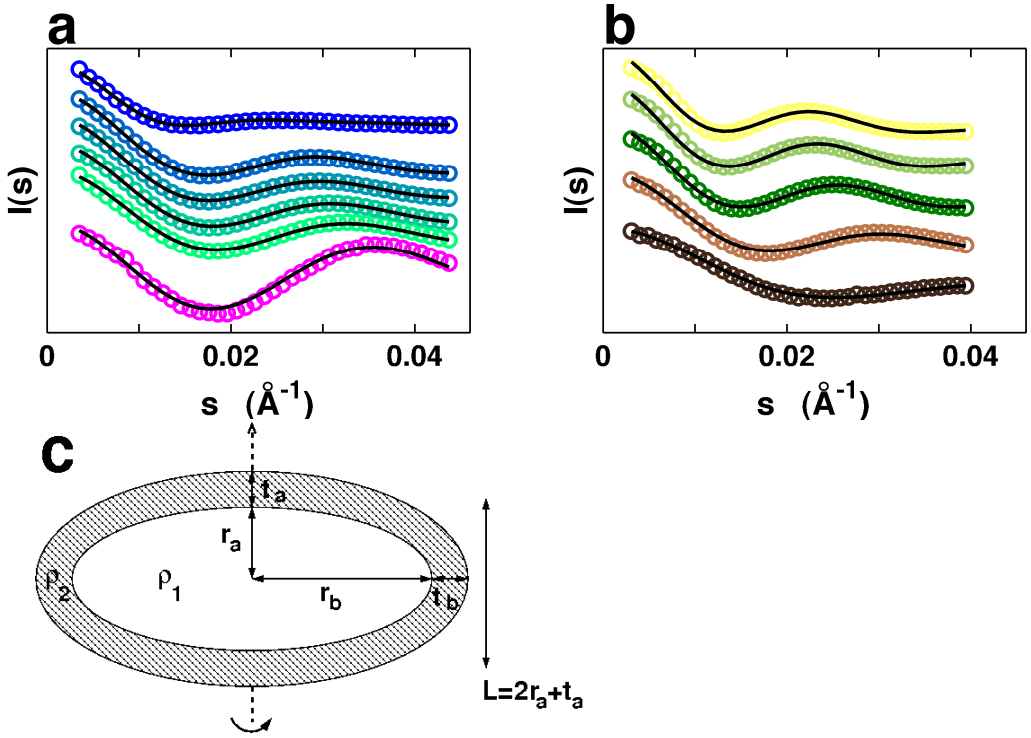

Experimental SAXS profiles for DDM/FC-10 (a) and DHPC/LPPG (b) micelles (circles, same color code as Figure S5) and fits with two-component ellipsoid models (black solid lines). Schematic of the two-component ellipsoid models (c) featuring an electron dense outer shell (corresponding to the head group region) and a less electron dense inner core (corresponding to the hydrophobic groups). The axis of rotation symmetry is shown as a dashed line. For oblate micelles, as shown in the panel c, the charactristic thickness L is given approximately by $L \approx 2r_a+t_a$ as annotated in the Figure. For prolate micelles (i.e. for micelles with $r_a > r_b$) the corresponding relationship is $L \approx 2r_b+t_b$. Details of the model and the fitting routine are as described in reference[5]. Fitting parameters are reported in Supplementary Table 3. The number of data points in the experimental scattering profiles was reduced for clarity.

Figure S6. SAXS data for the TM0026/DM protein-detergent complex.

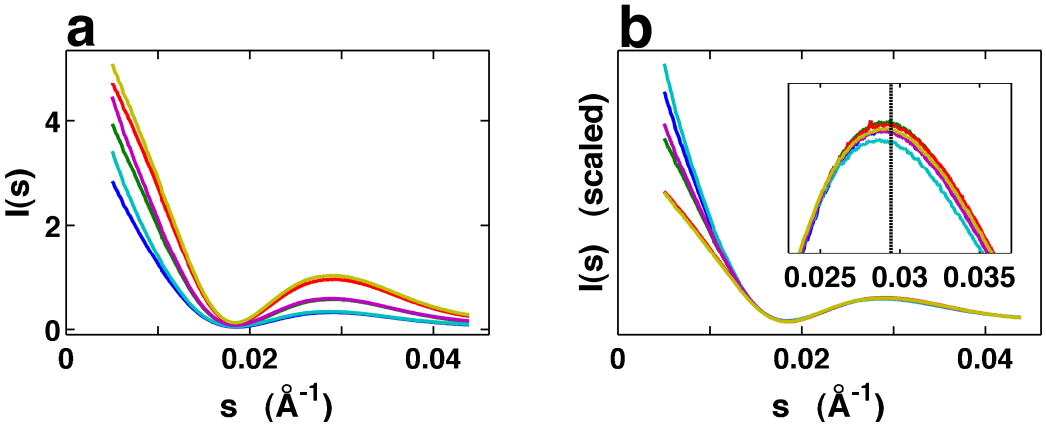

SAXS data for TM0026 in DM at different protein-detergent stoichiometries. Scattering profiles for 0.18 mM TM0026 in 88 mM DM (blue), 150 mM DM (green), 300 mM DM (red) and 0.36 mM TM0026 in 88 mM DM (cyan), 150 mM DM (magenta), 300 mM DM (yellow). Panel b) shows the same data as panel a), but after rescaling by the scattering intensity at high *s* to superimpose the second maximum in the scattering intensity for ease of comparison. The inset shows a close up of the same data around the second maximum. The vertical dashed black line indicates the position of the second peak for DM micelles in the absence of protein.

In principle, the SAXS profile of the protein-detergent complex is complicated by the additional electron density of the protein and, therefore, *L* is not as easily interpreted as in the case of "empty" micelles. However, for TM0026 in DM, the position of the second maximum in the scattering profile varies only slightly at different ratios of protein to detergent and is similar to the value observed for pure DM micelles (inset of panel b). This suggests that the characteristic distance *L* is similar in TM0026-DM protein detergent complexes and pure DM micelles.

Figure S7. The EPR spectra of TM0026 in DM and DDM/FC-10 micelles are identical.

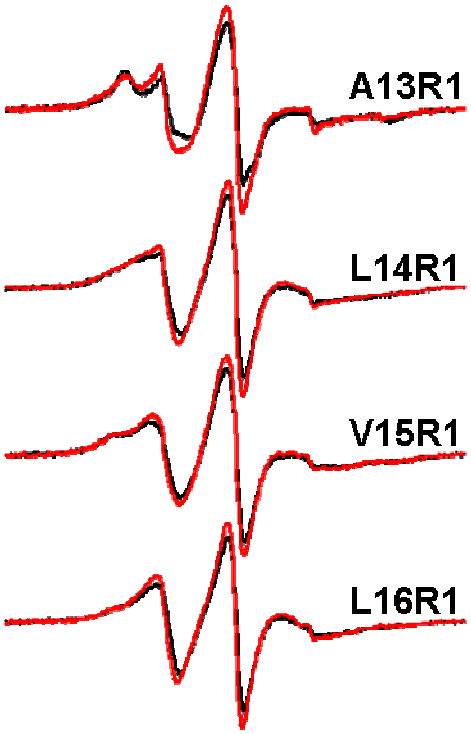

The EPR Spectra of A13R1 – L16R1 in DM (black) and the DDM/FC-10 mixed micelle (red). Similar to the results observed in the ^{15}N, ^{1}H-TROSY spectrum, the EPR spectra of the spin labeled mutants in the DDM/FC-10 mixed micelle are identical to the EPR spectra recorded in DM. Therefore, the structural heterogeneity of TM0026 in the FC-10 micelle is reversible.

Figure S8. TM0026 backbone chemical shift differences between DM and DDM/FC-10 mixed micelles.

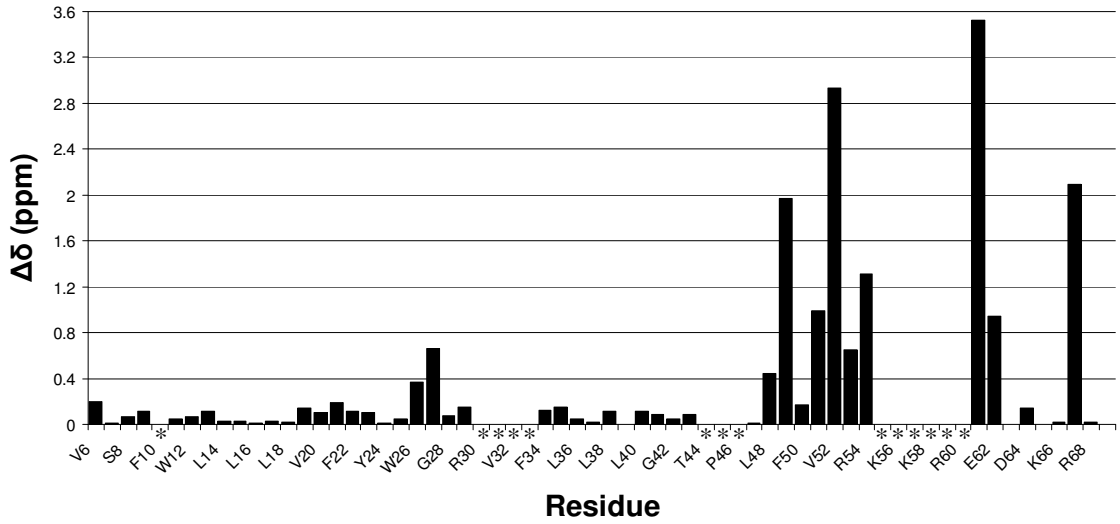

The chemical shift difference ($\Delta\delta = \sqrt{((\Delta\delta_N/5)^2+(\Delta\delta_H)^2)}$) between the DM and DDM/FC-10 detergent conditions is plotted for each residue that was assigned in both detergent conditions. The average shift is $\Delta\delta \approx 0.4$ ppm. Asterisks indicate that $\Delta\delta$ values could not be calculated because assignments were missing in one or both of the detergent conditions.

Figure S9. Interactions between TM0026 and DM detergent alkyl chains.

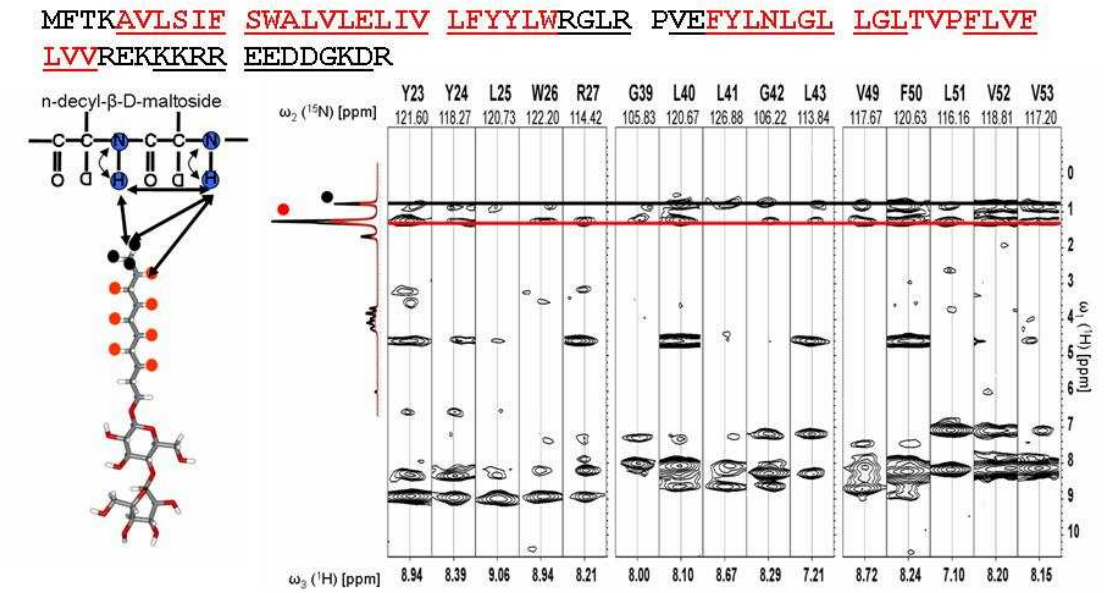

Select strips of a 3D ^{15}N-editted NOESY spectrum are shown. The 1D ^{1}H NMR spectrum of the DM micelle is shown to the left of the spectrum. The resonances that correspond to the DM alkyl chain are marked with a black circle and red circle. The resonances correspond to the chemical shifts similarly labeled on the structure of DM (left). The protein sequence is shown above with the transmembrane α-helices colored red and the assigned amino acids underlined.

Table S1. Dynamics parameters of spin labeled TM0026.

	DM	FC-10	DDM	FC-10/DDM
A13R1	4.8	2.5	4.5	4.6
L14R1	3.4	2.6	4.4	3.2
V15R1	3.9	2.9	4.6	3.6
L16R1	3.4	2.7	4.2	3.2

Comparison of ΔH_{pp} (Gauss) for the spin labeled mutants of TM0026. The values for FC-10 are all lower compared to the other detergent conditions indicating a highly dynamic sequence. The FC-10/DDM mixed micelle values are comparable to those measured in DM. The measurement of $2A_{zz}$ is difficult with multi-component spectra because the hyperfine peaks are broadened to the extent that a maximum and minimum can not be selected; however, a qualitative assessment allows a comparison of mobility.

Table S2. Detergent properties.

Detergent (Abbreviation)	Ionic property	CMC (mM)	L (Å)
n-decylphosphocholine (FC-10)	zwitterionic	11	28.0 ± 0.4
n-dodecylphosphocholine (FC-12)	zwitterionic	1.5	34.3 ± 0.6
n-decyl-β-D-maltoside (DM)	non-ionic	1.8	34.0 ± 0.4
n-dodecyl-β-D-maltoside (DDM)	non-ionic	0.17	39.8 ± 0.4
n-octyl-β-D-glucoside (OG)	non-ionic	18-23	27.0 ± 0.5
n-nonyl-β-D-glucoside (NG)	non-ionic	6.5	29.5 ± 0.5
n-decyl-β-D-glucoside (DG)	non-ionic	2.2	32.2 ± 0.5
1,2-dihexanoyl-sn-glycerophosphocholine (DHPC)	zwitterionic	14-15	22.4 ± 0.8
1-palmitoyl-2-hydoxy-sn-glycero-3-[phospho-rac-(1-glycerol)] (LPPG)	ionic	0.018	45.5 ± 1.2

Ionic properties, critical micelle concentrations (*CMC*) and characteristic head group-head group spacing across the micelle core (*L*) for selected detergents. *CMC* values are taken from the literature[5], values for *L* are determined from the position of the second peak in the scattering intensity[5].

Table S3. Geometrical parameters from two-component ellipsoid models for FC-10/DDM and DHPC/LPPG mixed micelles.

[FC-10] (mM)	[DDM] (mM)	χ_{DDM}	L (Å)	Shape	r_a (Å)	r_b (Å)	t_a and t_b (Å)	V_{HC} (nm^3)
50	0	0	28.4	Prolate	20.7-21.2	13.4-13.6	2.7-3.0	15
50	10	0.20	31.6	Oblate	12.5	20	3.0-3.5	19
50	25	0.39	33.6	Oblate	14	20.5	3.5	23
50	40	0.51	34.8	Oblate	14.0-14.5	22	3.5-4.0	25
50	50	0.56	35.4	Oblate	14.5-15.0	22.5	4.0-4.5	26
0	5	1	39.8	Oblate	14.0-14.5	28.0-29.5	6.0-6.3	49

[DHPC] (mM)	[LPPG] (mM)	χ_{LPPG}	L (Å)	Shape	r_a (Å)	r_b (Å)	t_a and t_b (Å)	V_{HC} (nm^3)
50	0	0	22.4	Prolate	20.5-22.5	9.5-10.5	3.0-4.0	9
40	10	0.26	28.6	Oblate	14.5-15.5	19.0	4.5-5.0	22.7
25	25	0.59	38.5	Oblate	19.0-20.0	21.0-22.0	4.5-5.5	37.0
10	40	0.85	43.4	Oblate	21.5-22.5	24.0-25.0	5.5-6.0	55.5
0	50	1.00	45.5	Oblate	19.0-20.0	29.5-30.5	5.5-6.0	73

The size and shape of FC-10/DDM and DHPC/LPPG mixed micelles determined from two-component ellipsoid fits (see **Supplementary Fig. 5**).

Supplementary References

(1) Columbus, L.; Hubbell, W. L. *Trends Biochem. Sci.* **2002**, *27*, 288-95.

(2) Columbus, L.; Kalai, T.; Jeko, J.; Hideg, K.; Hubbell, W. L. *Biochemistry* **2001**, *40*, 3828-46.

(3) Hubbell, W. L.; Cafiso, D.; Altenbach, C. *Nat. Struct. Biol.* **2000**, *7*, 735-739.

(4) Mchaourab, H.; Lietzow, M.; Hideg, K.; Hubbell, W. *Biochemistry* **1996**, *35*, 7692-7704.

(5) Lipfert, J.; Columbus, L.; Chu, V. B.; Lesley, S. A.; Doniach, S. *J Phys Chem B* **2007**, *111*, 12427-38.